Miniature Shape Memory Alloy Actuator for Tactile Binary Information Display

Ramiro Velázquez, Edwige Pissaloux and Jérôme Szewczyk
Laboratoire de Robotique de Paris, CNRS FRE 2507
18 Route du Panorama, BP 61,
92265 Fontenay aux Roses, France
{velazquez, pissaloux, sz}@robot.jussieu.fr

Moustapha Hafez
CEA/LIST
18 Route du Panorama, BP 61,
92265 Fontenay aux Roses, France
moustapha.hafez@cea.fr

***Abstract* - This paper presents a new miniature actuator, which is currently being used to design and develop high resolution, lightweight and compact interfaces for tactile binary information representation such as Braille. Since the main drawback of these devices is their high cost, the proposed actuator exploits the simplicity of its design to provide a low-cost actuation alternative. Based on shape memory alloy (SMA) technology, the actuator consists of an antagonist arranged pair of NiTi helical springs. The actuator of 1.5 mm diameter and 150 mg weight is capable of developing a 320 mN pull force and 1.5 Hz bandwidth by using simple forced-air convection. A combined computational/experimental study on the thermomechanical properties of both SMA active element and actuator is presented to evaluate characteristics such as actuation speed, force and stroke. In conclusion, the prototype and performance results are reported and discussed.**

Index Terms - SMA, NiTi helical spring, tactile actuator (taxel), antagonist behavior.

I. Introduction

Tactile displays are devices meant to stimulate the skin, particularly on fingertips, to create sensations of contact. Such devices have for a long time been the domain of developments for visual information transmission for the visually impaired: reading (Braille characters) and graphic/pictorial representation of some 2D scenes. More recently, this field has expanded to include potential uses in virtual reality, sensory augmentation, sensory substitution, tele-surgery, robotics among many others.

Typical displays involve arrays of upward/downward moveable pins as skin indentation mechanisms. Most devices commercially available are piezoelectric Braille displays. A Braille cell (eight contact pins), which represents a single character, costs around 40 USD and about 80 cells are typically used for displaying a line of text [1].

Cost is not the only drawback when further applications of a significant number of Braille cells are envisaged. As piezoelectric technology is limited in stroke, mechanical amplifiers are needed. These are implemented as an additional burdensome module attached to the contact pins (Figure 1(a)). Displaying more than 2 lines of text at a time or 2D graphics becomes practically impossible: only two cells are possible to be arranged vertically (Figure 1(b)).

More suitable devices for 2D tactile graphics have emerged but few have had an industrial development. A successful example is Metec's DMD-12060 display based on miniature solenoids, which offers a 159 x 59 array for 70,000 USD [1].

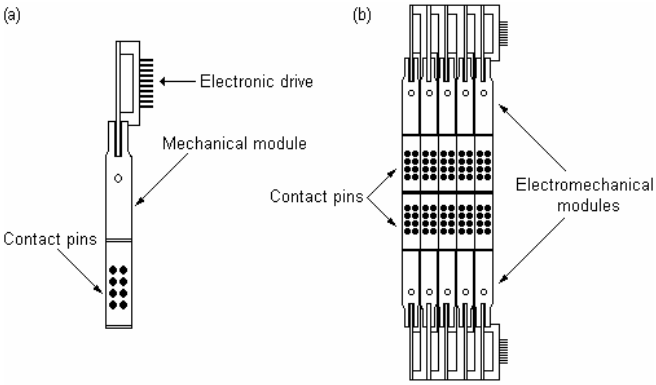

Fig.1. (a) Braille cell and (b) Braille cells vertical arrangement.

Undoubtedly, there is still a great interest in new actuators for tactile applications that allow a more efficient implementation in terms of cost, performance and flexibility.

Actuation techniques already explored include servomotors [2], electromagnetic coils [3], piezoelectric ceramics [4], pneumatics [5], shape memory alloys (SMA) [6], polymer gels [7] and fluids technologies [8]. Each of these approaches has its own advantages/disadvantages and none of them has been found optimal for tactile displays.

SMA technology is one of the most promising candidates for high resolution tactile displays. Advantages like simplicity, compactness, high power/weight ratio, noiseless operation, extremely high fatigue resistance to cyclic motion and low-cost make them an interesting actuation principle. However, reported results [6], [9], [10], [11] indicate small strokes due to a low 4 to 5% shape memory strain, high electrical heating current (2 A), slow response using forced-air convection (up to 1 Hz) and the need of miniature mechanical clamping structures to keep the SMA active without power supply.

A SMA based miniature actuator that seems to improve characteristics such as cost, integration capacity and overall performance will be presented in this paper. The rest of the paper is organized as follows: Section 2 presents a brief review of human tactile perception and the requirements for an efficient tactile actuator (taxel). Section 3 introduces the NiTi helical spring and evaluates its thermomechanical properties for actuation. Section 4 describes the actuator's design concept and characterization, while section 5 presents and discusses the prototype and its performance. Finally, section 6 concludes with main remarks and future work perspectives.

II. TACTILE PERCEPTION AND REQUIREMENTS FOR TACTILE STIMULATORS

Physiology of touch shows that mainly Meissner and Pacini skin mechanoreceptors are involved in hand feeling during object exploration. While Pacini cells are sensitive to high frequency vibration, Meissner ones are sensitive to low frequency fine-touch stimuli [12]. It seems that Meissner cells are mainly involved in surface gradient information registration.

Meissner cells in fingertips are located in a 0.7 mm depth from the surface and there are as many as 140 per cm². This corresponds to a 0.9 mm center-to-center spacing. However, this does not mean that we can actually perceive with this resolution. Human touch cannot perform discretely below a resolution suggested by a two-point discrimination threshold (TPDT). The TPDT is the minimum distance with which we can identify 2 points given in a simultaneous two-point-contact [12]. The TPDT on fingertips is 2 to 3 mm, being 2.54 mm the standard TPDT adopted by Braille devices. On the other hand, a survey of psychophysical experimental data [13] indicates that a 50 to 100 mN force is applied during a fine-touch object exploration.

Mechanical requirements for touch stimulation require then to integrate a wide number of micro-actuators with a 2.54 mm interspacing, an effective skin indentation of 0.7 mm and a minimum deliver force of 100 mN.

III. SHAPE MEMORY ALLOY ACTIVE ELEMENT

Shape memory alloys can be formed into almost any shaped actuator. Most popular shapes are wire, spring, tubing, sheet and ribbon.

Experimental testing of NiTi SMA straight wires has revealed that stroke is limited to approximately 4 to 5 % of their original length.

Compared to wires, springs do have a significantly higher recoverable strain. Impressive 300% strokes can easily be obtained using helical springs. However, as they perform in torsion instead of tension, they cannot develop the same force.

This paper suggests that SMA springs can be designed to exert significant forces for touch applications having at the same time, stroke and compactness not offered by straight wires.

A. Material

A NiTi helical spring was fabricated with trademark Flexinol wire with the following geometric characteristics: 200 μm of wire diameter, 1.5 mm of spring outer diameter and 12 active coils.

Energy dispersive x-ray (EDX) analysis confirmed its composition to be approximately $Ni_{52}Ti_{48}$. The helical spring shape was set through a heat treatment process in which the material was subjected to 500°C for 5 minutes. Rapid cooling via water quench concluded the process.

The stable transformation temperatures determined by differential scanning calorimeter (DSC) are 65, 28, 59, 36, -3 and -37°C for A_f, A_s, R_s, R_f, M_s and M_f, respectively.

B. Evaluation of SMA thermomechanical properties

1) Deformation properties: The deformation behavior of a SMA is based on a rearrangement of its crystalline structure due to a phase transformation process. At a macroscopic level, it determines the force and motion developed by the SMA element.

Considering the simple geometry of a helical spring, Tobushi and Tanaka [14] have proposed an elastoplastic constitutive relation to predict its SMA force-deflection behavior. This relation suggests a stress-strain-temperature dependence which can be written as:

$$F = \begin{cases} \dfrac{Gd^4}{8ND^3}\delta & \text{for } \delta < \delta_e \\ \dfrac{\pi\tau_p d^3}{6D}\left[1-\dfrac{1}{4}\left(\dfrac{\pi N\tau_p D^2}{dG\delta}\right)^3\right] & \text{for } \delta \geq \delta_e \end{cases} \quad (1)$$

$$\text{with: } \delta_e = \frac{\pi D^2 N\tau_p}{Gd} \text{ and } \tau_p = \begin{cases} c_M(T-M_S) & \text{for loading} \\ c_A(T-A_S) & \text{for unloading} \end{cases}$$

where F is the force developed by the SMA spring as a function of deflection δ, d is the wire's diameter, D is the mean spring diameter, N is the number of active coils, G is the shear modulus of elasticity, τ_p the temperature dependent torsional stress, δ_e is the boundary of elastic and plastic regions and c_M, c_A are material's constants which describe the transformation conditions.

For NiTi, the experimental data in [14] indicate austenitic G=28.2 GPa and martensitic G=10.5 GPa and estimate c_M = 6.3 MPa/K and c_A = 4.9 MPa/K.

Figure 2(a) compares the calculated and experimental force-deflection curves under various isothermal conditions for a maximum deflection of 10 mm. Experimental loading/unloading results were obtained from tensile tests.

As seen, numerical results well explain the spring's overall deformation behavior. The loading curves indicate that the maximum output force of the SMA spring at a deflection of 10 mm is approximately 180 mN at 20°C, 410 mN at 85°C and 720 mN at 105°C. On the other hand, the unloading curves indicate the mechanical hysteresis of the SMA when the original configuration is being recovered. Note that for temperatures at or above the austenite state, the memory shape is perfectly recovered but for martensite ones, it does not.

Figure 2(b) confirms the presence of the R-phase. According to the DSC analysis, martensite phase takes place within the range -3 to -37°C. This means that, for actuation at room temperature, the M-transformation will never occur. The use of the R-phase instead of the M-phase will be neglected for this work as the R-hysteresis is as small as 1 mm. Figure 2(c) shows the phenomenological representation of the spring's SMA behavior in the force-deflection-temperature space.

2) Actuation speed: As aforementioned, the deformation behavior of SMAs is based on rearrangement of crystalline structure due to a phase transformation. This

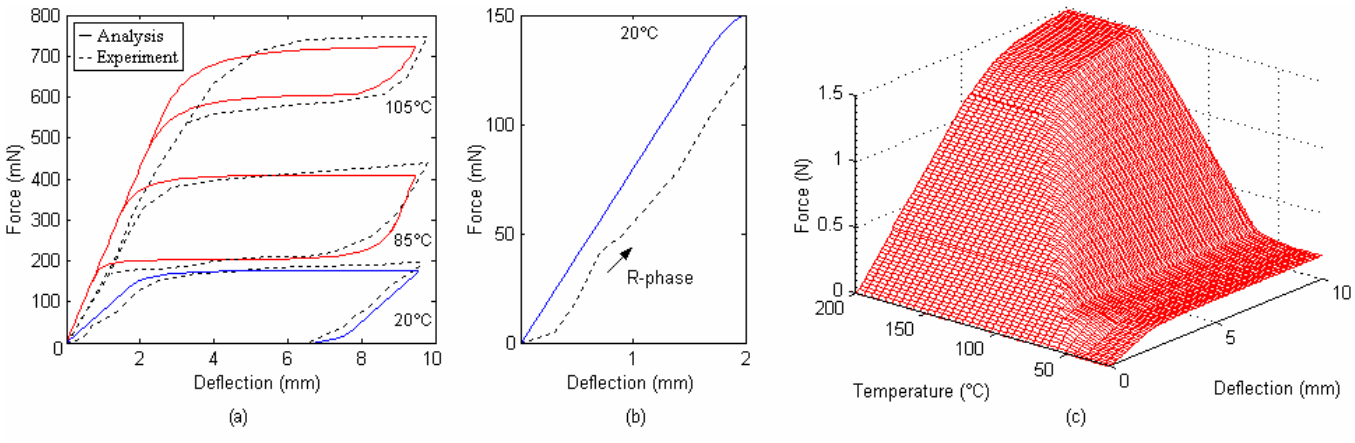

Fig.2. Deformation behavior of the SMA spring: (a) Force-deflection relations at constant temperatures (20°C, 85°C and 105°C), (b) hysteresis due to R-phase and (c) computational SMA behavior in the force-deflection-temperature space.

phenomenon is thermally driven: it triggers once the SMA passes from martensite (or low temperature phase) to austenite (or high temperature phase).

In this paper, thermal dynamics of a SMA is defined by Ikuta's heat transfer constitutive model [15] and Liang and Roger's kinetics law [16]. These equations can be summarized as follows:

$$\rho V\left[C\frac{dT}{dt}+\Delta H\frac{d\eta}{dt}\right]=\begin{cases}Ri^2-hS(T-T_e) & \text{(heating)}\\ -hS(T-T_e) & \text{(cooling)}\end{cases} \quad (2)$$

where ρ is the density of the SMA, V is the volume of the material, C is its specific heat capacity, R is the electrical resistance, i is the heating current applied, h is the heat transfer coefficient, S is the surface area of the SMA and T_e is the environment's temperature (20°C).

Concerning Liang and Roger's ΔH dη/dT phase transformation term, the amount of martensite fraction η transformed on a temperature T can be written for cooling as:

$$\eta(T)=\begin{cases}0 & \text{at } T > M_S\\ \frac{1}{2}\left[\cos\left(\pi\frac{T-M_f}{M_S-M_f}\right)+1\right] & \text{at } M_f < T < M_S\\ 1 & \text{at } T < M_f\end{cases} \quad (3)$$

The analogous dependence can be expressed for heating by replacing M_s and M_f temperatures with A_f and A_s temperatures correspondingly.

Thermal properties of NiTi extracted directly from Flexinol technical data sheets are specified in table 1.

Table 1. Thermal specifications of the NiTi spring.

Property	Value	Unit
Density ρ	6.45	g/cm³
Specific heat C	0.32	J/g°C
Latent heat ΔH	14.38	J/g

One of the major problems when SMAs are electrically heated is the non-linearity of their electric resistance. It is widely known that resistivity in NiTi alloys changes its value from martensite to austenite. Additionally to this temperature dependence, electric resistance in SMAs has also been found strain-dependent.

Figure 3 shows both springs' measured electric resistance and force as a function of strain. Tests were conducted at room temperature for a maximum deflection of 10 mm. Note that resistance increases with deflection.

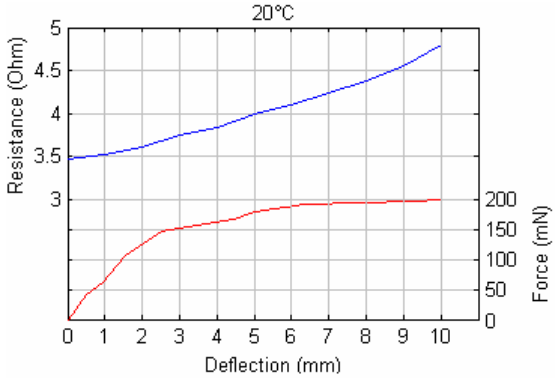

Fig.3. The upper curve shows the spring's measured electric resistance as a function of its deflection and the bottom curve shows the corresponding force developed.

Experimental results on the spring's thermal behavior could not be performed using a temperature sensor: typical commercially available thermocouples offer sample rates up to 0.6 s; too low for measuring a rapid evolution of temperature. Instead, a relation between displacement and temperature was performed using a 20 ms sample rate linear variable differential transformer (LVDT).

As seen in figure 4(a), a set of heating current is applied to a 3 mm pre-strained spring under free-convection conditions (h=6 W/m²°C). The amplitude is varied from 200 to 500 mA. Recall from theory that a SMA heated from cold begins to transform into the austenite phase at a temperature called *austenite start* A_s, and its transformation is essentially complete at a temperature called *austenite finish* A_f. Consequently, the time in which the SMA starts to present deformation is exactly the time that it needs to heat enough to reach A_f.

Figure 4(b) bottom presents a zoom of the interest area while the top section shows the analytical temperature evolution in the austenite phase. Results are compared in table 2.

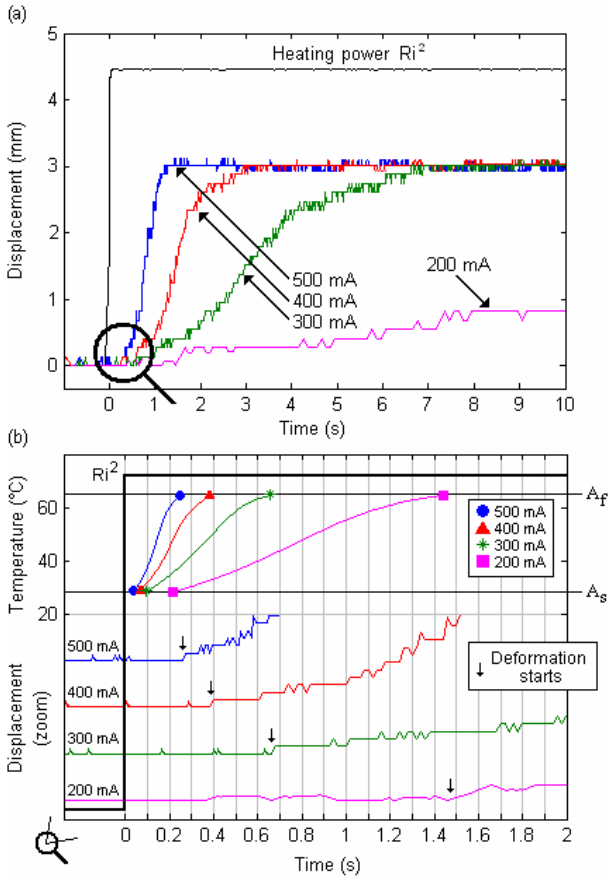

Fig.4. Time response using a displacement relation: (a) Response to a set of input current (3 mm pre-strained spring) and (b) analytical/experimental comparison of actuation times.

Table 2. Comparison of analytical/experimental actuation times.

Heating current (mA)	Time (s)		
	Calculated		Experimental
	A_s	A_f	
500	0.0341	0.2387	0.26
400	0.0532	0.3712	0.38
300	0.0947	0.6536	0.66
200	0.213	1.4313	1.46

Despite of the rough assumptions made on the thermal properties of NiTi, the analytical results reproduce sufficiently close the experimental actuation speed.

IV. SMA TACTILE ACTUATOR

SMAs can be used to design actuators that create linear motion. We propose a new SMA based electrically driven taxel. The idea we have developed simply consists of a pair of SMA springs configured in antagonist mode. The operation principle is shown in figure 5.

At the initial position (1), the actuator's contact pin is raised. Both SMA springs are unstressed and in martensite phase, (2) when the SMA spring-1 is electrically heated, it recovers an austenitic compressed memorized shape that extends the SMA spring-2 and retracts the contact pin. The taxel is now in the lower position. (3) When the electrical current is disconnected, the temperature of the spring-1 starts to decrease and so its yield strength. In consequence, the contact pin tends to rise. However, it will be demonstrated that it does not return to the initial position (pin raised); the lower position is still assured. (4) To raise again the pin, SMA spring-2 is activated. Upon cooling, the initial position will be reached.

Consider now the case when the surface is explored with the fingertips; (5) as seen in (1), the taxel's default configuration is when both springs are in martensite phase and the contact pin is raised. This configuration withstands up to a contact force of 120 mN (a normal haptic exploration). (6) If the user applies a higher force (an intentionally violent touch), the contact pin will be retracted to surface level. (7) When the force is released, the contact pin naturally rises to recover its original configuration.

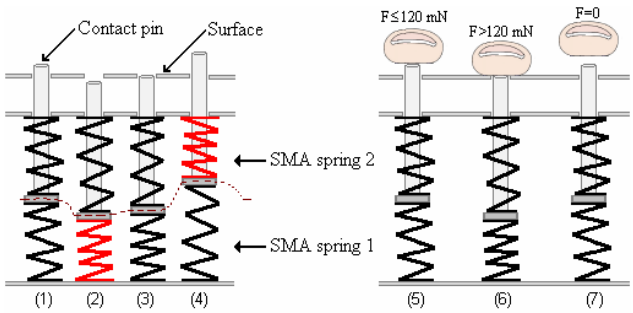

Fig.5. Principle of the SMA tactile actuator (taxel).

The three main advantages of this concept are:

• A symmetric dynamic behavior (as both SMA springs are identical).

• The actuator needs only energy when changing from one state to the other. In neither of two end positions energy is needed.

• No miniature mechanical clamping structures are needed to keep the taxel active. Lower and higher positions are assured by the mechanical characteristics of the SMA springs.

Let us characterize the actuator's SMA antagonist behavior using a pair of SMA springs of geometric and thermomechanical characteristics described so far.

Consider both springs identically pre-strained (distance O-δ_0 and O'-δ_0 in figure 6(a)) in martensitic equilibrium point δ_0 (Figure 6(a.1)). When the lower spring is heated, the new equilibrium point B is defined by the intersection of its austenite curve and the upper spring's martensite one (Figure 6(a.2)). When cooling, the lower spring tends to recover its martensite characteristic at the same time that the upper one mechanically unloads. As seen, the equilibrium point does not follow the B-δ_0 trajectory but the B-D one (Figure 6(a.3)). The same phenomenon is observed when the upper spring is heated; it follows δ_0/D-A-C instead of δ_0/D-A-δ_0 (Figures 6(a.4) and 6(a.5)).

A more complete representation of the thermomechanical path followed by the equilibrium point is shown in figure 6(b). Note that the initial position δ_0 is not recovered due to the mechanic unloading characteristic of martensite.

Let us analyze the case when an external force is applied to the system. Two situations are to be predicted:

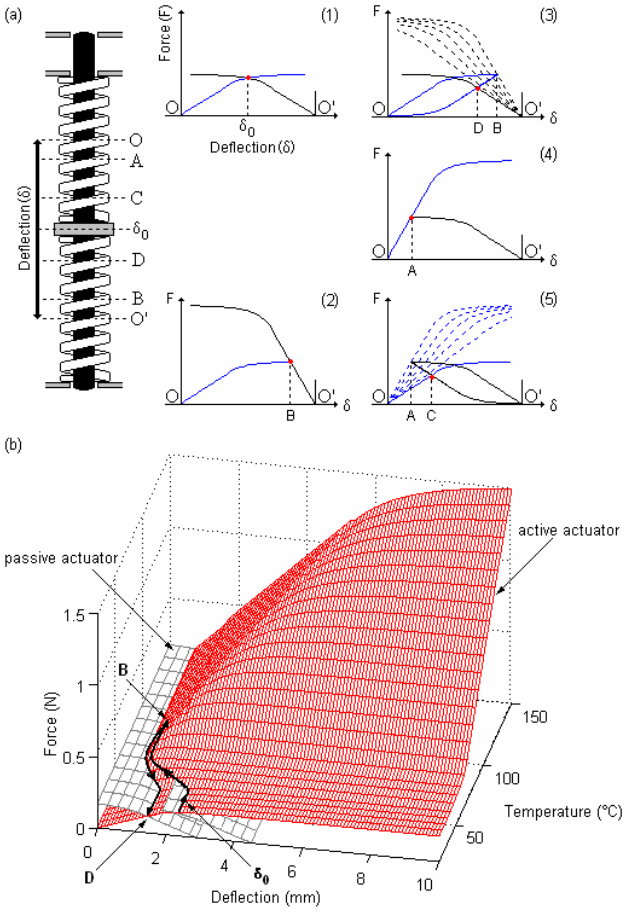

Fig.6. The actuator's SMA antagonist principle: (a) the actuator's conceptual representation and force-deflection relations for a complete operating cycle. (b) Thermomechanical path performed by a spring in the force-deflection-temperature space.

1) The force is applied during the austenitic state of the upper spring (Figure 7(a.1)). The superelasticity property appears in active spring while the passive one follows an unloading behavior. Note that a 320 mN force is needed to reach point δ_0 (Figure 7(a.2)). When the external force is released, the active spring unloads by following its austenite characteristic as the passive one mechanically loads (Figure 7(a.3)).

Figure 7(a.4) shows this thermomechanical path in the force-deflection-temperature space. Note that the initial position *A* is recovered in this case even though a non-reversible path is observed between A-δ_0.

2) The force is applied during the martinsitic state of the upper spring (Figure 7(b.1)). Note that, while the upper spring follows a loading behavior, the passive one performs an unloading path. A 120 mN force is required in this case to reach point δ_0 (Figure 7(b.2)). When the external force is released, both springs mechanically unload by following their martensite characteristic (Figure 7(b.3)). Note that point *C* is not recovered.

Figure 7(b.4) shows the force-deflection path performed for martensitic temperatures. Note that a new point *E* appears after the force is released. For subsequent cycles, a 60 mN force is required to reach δ_0 from point *E*.

In conclusion, pre-stain δ_0 must be carefully determined in order to calibrate the system and assure that *B* and *D* positions will provide a lower taxel position while *A*, *C* and *E* will provide an upper one. Pre-straining both springs 2.3 mm at installation satisfies these requirements.

V. Prototype and Performance

Figure 8 shows the prototype actuator built with an antagonist arranged pair of NiTi springs. The actuator is 1.5 mm diameter, 45 mm length and 150 mg weight. Its laboratory cost is 2 USD.

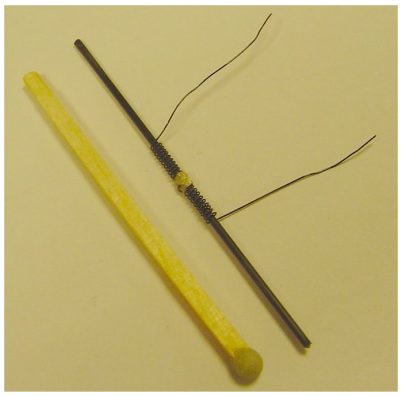

Fig.8. SMA miniature tactile actuator.

As mentioned, phase transformation of SMAs is thermally driven, being limited by the speed with which they can be heated and cooled. As table 2 suggests, it is always possible to apply more electrical current to produce a faster response. The fundamental limitation is cooling.

Several approaches [9], [17] have suggested the use of water and heat sinking mechanisms as coolants. It has to be recognized that these methods have shown the most promising results. However, an actuator immersed in constant recirculating water and additional mechanisms complicate the actuator's design and hardly imply a fully portable, lightweight and compact tactile display.

To keep the actuator's simplicity, forced-air convection provided by a regular computer mini-fan was used as cooling system. Figure 9 shows the experimental set-up and tracking response of the antagonist actuator, under no-load conditions, to a 1.5 Hz square power signal.

Note that one of the constraints of the actuator is that at no time should both SMA springs be driving the system. For this purpose, an inverse switch was used to route the input and alternatively activate springs 1 and 2.

As seen, a 6.8 W power signal (a 1.3 A heating current) is applied to each spring under forced-air cooling conditions to obtain the actuator's 3 mm total stroke (distance *A*-*B*).

VI. Conclusion

This paper has presented a SMA based electrically driven miniature actuator intended for tactile stimulation. This actuator uses an antagonist arranged pair of SMA NiTi helical springs, which thermomechanical properties have been analytically and experimentally presented to

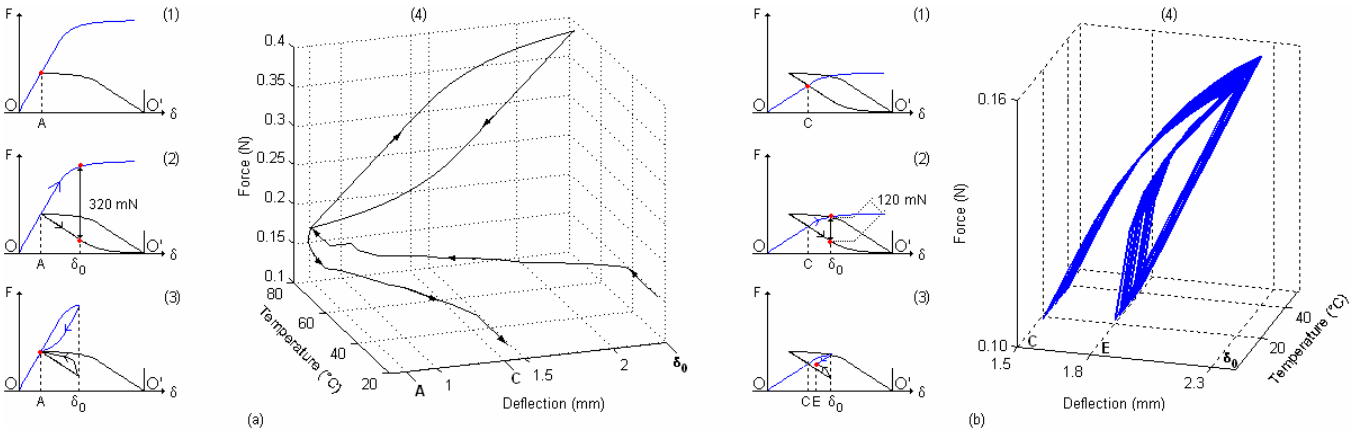

Fig.7. The upper spring's behavior face to an external force: (a) austenitic and (b) martensitic cases.

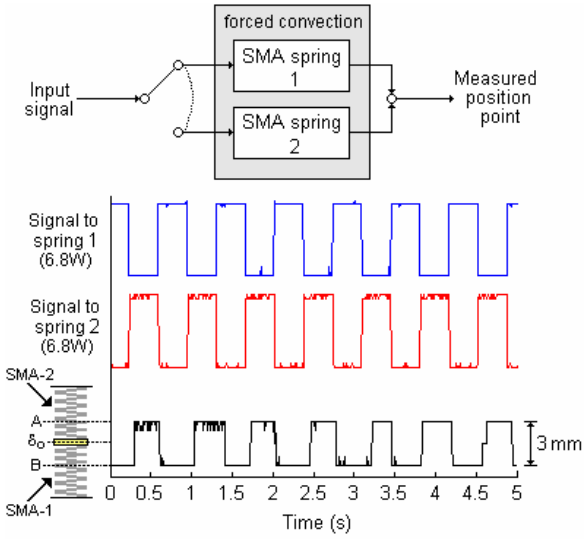

Fig.9. Tracking response of the actuator to a 1.5 Hz power signal.

characterize the actuator's antagonist type behavior and performance.

The taxel of 1.5 mm diameter, 45 mm length, 150 mg weight and 3 mm total excursion is capable of producing an effective 0.7 mm skin deformation with a 320 mN pull force at 1.5 Hz bandwidth.

The main advantages of this actuator are:

• The simplicity of its design: no clamping structures are used to keep the SMA elements active. In the worst case, the active position is assured by a 60 mN pull force.

• Its overall performance: A more modest current level (1.3 A) is used to obtain a higher bandwidth (1.5 Hz) by using forced-air convection provided by a simple and inexpensive mini-fan.

• Its low cost.

Ongoing work is now completely focused on its implementation to the development of a high resolution, lightweight, low-cost and compact tactile display. Fig. 10 shows a conceptual representation of an 8 x 8 array tactile display.

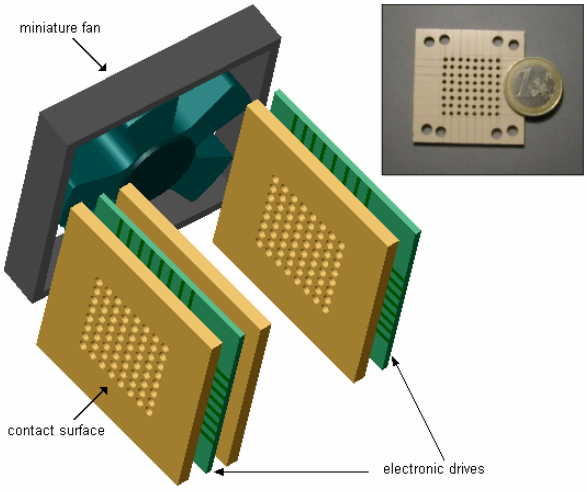

Fig.10. Conceptual representation of a 8 x 8 SMA based tactile display.

REFERENCES

[1] National Federation for the Blind, http://nfb.org

[2] C. Wagner, S. Lederman and R. Howe, "A tactile shape display using RC servomotors", *Proc. of the 10th Symp. on haptic interfaces for virtual environment and teleoperator syst.,* Orlando, USA, 2002.

[3] M. Benali-Khoudja et al., "Electromagnetically driven high-density tactile interface based on a multi-layer approach", *Proc. of the 2003 IEEE-MHS*, Nagoya, Japan, pp 147-152, 2003.

[4] J. Pasquero and V. Hayward, "STReSS: A practical tactile display system with one millimeter spatial resolution and 700 Hz refresh rate", *Proc. of Eurohaptics 2003*, Dublin, Ireland, pp 94-110, 2003.

[5] G. Moy, C. Wagner and R. Fearing, "A compliant tactile display for teletaction", *Proc. of IEEE-ICRA*, Piscataway, USA, 2000.

[6] P. Taylor, A. Moser and A. Creed, "A sixty-four element tactile display using SMA wires", *Elsevier Science BV*, pp 163-168, 1998.

[7] R. Voyles et al., "Design of a modular tactile sensor and actuator based on an electror-heological gel", *Proc. of IEEE-ICRA*, 1996.

[8] P. Taylor et al. "An electrorheological fluid based tactile array for virtual environments", *Proc. of IEEE-ICRA*, 1996.

[9] P. Wellman et al., "Mechanical design and control of a high-bandwidth SMA tactile display", *Proc. of ISER*, Barcelone, 1997.

[10] R. Featherstone and H.Teh, "Improving the speed of SMA actuators by faster electrical heating", *Proc. of ISER,* Singapore, 2004.

[11] W. Brenner et al., "Micro-Actuation principles for high-resolution graphic tactile displays", *Proc. of ACTUATOR*, Bremen, 2000.

[12] S. Geiger, *Handbook of Physiology section 1: The Nervous System*, American Physiological Society, 1984.

[13] J. Loomis, "On the tangibility of letters and Braille", *Perception and Psychophysics*, 29(1), pp 37-46, 1981.

[14] H. Tobushi and K. Tanaka, "Deformation of a SMA helical spring", *JSME International Journal*, Series I, 34(1), pp 83-89, 1991.

[15] K. Ikuta, M. Tsukamoto and S. Hirose, "Mathematical model and experimental verification of SMA for designing micro-actuator", *Proc. of IEEE- MEMS,* pp 103-108, 1991.

[16] C. Liang and C. Roger, "One-dimensional thermomechanical constitutive relations for shape memory materials", *Journal of Intelligent Materials, Syst. and Structures,* 1(2), pp 207-234, 1990.

[17] R. Russell and R. Gorbet, "Improving the response of SMA actuators", *Proc. of IEEE-ICRA*, Nagoya, pp 2299-2304, 1995.